*Review*

# Understanding the Catalytic Activity of Microporous and Mesoporous Zeolites in Cracking by Experiments and Simulations

**Shih-Cheng Li** [ID], **Yen-Chun Lin** [ID] **and Yi-Pei Li** *[ID]

Department of Chemical Engineering, National Taiwan University, Taipei 10617, Taiwan; f08524007@ntu.edu.tw (S.-C.L.); r10524074@ntu.edu.tw (Y.-C.L.)
* Correspondence: yipeili@ntu.edu.tw

**Abstract:** Porous zeolite catalysts have been widely used in the industry for the conversion of fuel-range molecules for decades. They have the advantages of higher surface area, better hydrothermal stability, and superior shape selectivity, which make them ideal catalysts for hydrocarbon cracking in the petrochemical industry. However, the catalytic activity and selectivity of zeolites for hydrocarbon cracking are significantly affected by the zeolite topology and composition. The aim of this review is to survey recent investigations on hydrocarbon cracking and secondary reactions in micro- and mesoporous zeolites, with the emphasis on the studies of the effects of different porous environments and active site structures on alkane adsorption and activation at the molecular level. The pros and cons of different computational methods used for zeolite simulations are also discussed in this review.

**Keywords:** mesoporous materials; zeolite; density functional theory; catalytic activity

## 1. Introduction

Zeolites are microporous aluminosilicates with high surface area and crystallinity. They have been widely applied in many different fields, such as gas storage, water treatment, biomass upgrading, and oil refining, because of their strong acidity, excellent catalytic activity, shape selectivity, and hydrothermal stability. In the past decades, one of the most important applications of zeolites is in fluidized catalytic cracking (FCC) in the petrochemical industry, which accounts for more than 95% of the global zeolite catalyst consumption [1]. It is reported that 400 million tons of olefins are produced annually, and about 59% of olefins are produced by FCC units [2]. Light olefins are critical building blocks in the petrochemical industry, and the demand for olefins and their derivatives has continuously increased over the last decade [3,4]. Therefore, it is important to understand how to improve the catalytic performance of zeolites. Studies have shown that the performance of zeolite catalysts for cracking reactions is determined by various factors, including the porous size and composition, e.g., the Si/Al ratio and the presence of other heteroatoms or extra-framework aluminum (EFAL) species [5–12]. Since the range of possible combinations of zeolite structures and compositions is exceedingly large, it is highly desirable to understand the effects of zeolite topology and composition on hydrocarbon cracking in order to improve their activity and selectivity to desired products.

When silicon in a zeolite framework is substituted by a trivalent atom, such as Al, a cationic species is required to keep the framework charge neutral. If this cationic species is a proton, this chemical substitution generates a Brønsted acid site, which can activate C–C bond cleavage. Due to the importance of hydrocarbon cracking in the production of transport fuels, the influences of zeolite topologies, Si/Al ratios, and Al distributions on the adsorption and activation of hydrocarbons have been extensively studied by both experiments and computer simulations [6–10,13–23]. Various approaches have been developed to improve the performance of zeolite catalysts. For example, the cracking products

in conventional zeolites would be stuck in the micropores as a result of diffusion limitation, and therefore would be over-cracked into undesired byproducts, leading to coke formation and the subsequent deactivation of the catalysts. This problem can be alleviated by implementing mesopores in zeolites [24–28]. Studies have shown that hydrothermal treatment can be applied to remove Al from zeolite frameworks to create mesopores, which can eliminate the influence of micropore blockage and prevent catalyst deactivation by reducing coke formation [29–33]. In addition, hydrothermal treatment can lead to the formation of EFAL species in zeolites, which have been shown to enhance the acidity of nearby Brønsted acid centers, and hence could affect cracking activity [5,29,34–42]. Therefore, investigating the zeolite topologies and the structures and locations of aluminum species in zeolites is crucial to understanding the variations in cracking activity with different zeolite systems.

Recent advances in density functional theory (DFT) calculations also aid in understanding of detailed chemistry of catalytic reactions in zeolites. These calculations can be performed by either using periodic or cluster models. Periodic models can capture the interactions from the extended framework structures; however, performing periodic DFT simulations for zeolite systems is often computationally demanding due to the need for large unit cells [43]. On the other hand, using small cluster models can significantly reduce computational costs, but the unphysical boundary effect may lead to inaccurate results. To address these issues, recent studies have adopted the hybrid quantum mechanics/molecular mechanics (QM/MM) method, in which only a small cluster encompassing the active center is described by quantum mechanics, while the rest of the zeolite framework is described by a classical force field. This hybrid scheme can take into account long-range van der Waals and electrostatic interactions in porous environments without significantly increasing computational costs [43,44]. Nevertheless, low-frequency modes correspond to translational and rotational motions between alkanes and zeolites must be handled properly to derive accurate enthalpies and entropies. These low-frequency motions of weakly bound molecules are notoriously difficult to model because their potential energy surfaces are usually highly anharmonic [45]. Therefore, recent works have adopted various computational approaches, such as the mobile block Hessian method (MBH) [46], quasirigid rotor harmonic oscillator (quasi-RRHO) [47], and configurational-bias Monte Carlo (CBMC) [13] to better model the adsorption and activation of alkanes in zeolites.

In this review, we offer a summary of progresses and achievements of recent theoretical and experimental studies in alkane cracking occurring in micro- and mesoporous zeolites, with the emphasis on the effects of different pore topologies and active site structures on alkane activation and adsorption. The influence of zeolite structures on adsorption thermodynamics and alkane monomolecular cracking kinetics are discussed in Section 2. Subsequently, the effects of the incorporation of mesoporosity into zeolites are investigated in Section 3. Finally, active site structures that have been proposed such as Brønsted acidic protons and extra-framework species are summarized in Section 4.

## 2. The Effects of Zeolite Structures on Alkane Cracking

The influences of zeolite structures on cracking activity and selectivity are usually attributed to the confinement effects in zeolites, which can be studied by examining the variations in the parameters of alkane adsorption and activation with zeolite topologies [9,10,13]. In principle, the intrinsic activation enthalpies and entropies ($\Delta H_{int}^{\ddagger}$ and $\Delta S_{int}^{\ddagger}$) need to be calculated by subtracting the adsorption thermodynamic properties ($\Delta H_{ads}^{\ddagger}$ and $\Delta S_{ads}^{\ddagger}$) from the apparent activation enthalpies and entropies ($\Delta H_{app}^{\ddagger}$ and $\Delta S_{app}^{\ddagger}$) derived from kinetic data measured experimentally, so an accurate determination of adsorption enthalpies and entropies is required to determine intrinsic catalytic activities. However, it is difficult to experimentally measure alkane adsorption enthalpies and entropies at cracking conditions (>673 K), so the adsorption properties of alkanes have been evaluated using theoretical calculations [9,13].

For example, Bell and coworkers demonstrated that $\Delta H_{ads}^{\ddagger}$ and $\Delta S_{ads}^{\ddagger}$ can be calculated accurately using CBMC simulations, which can properly capture the redistribution of adsorbed alkanes to different active sites [9,13]. Janda et al. calculated the adsorption

parameters for propane, butane, pentane, and hexane in H-MFI at the T4 and T9 positions, which are located in the sinusoidal channel and at the channel intersection, respectively [13]. As shown in Figure 1, the $\Delta H^{\ddagger}_{ads}$ and $\Delta S^{\ddagger}_{ads}$ are more negative for T4 than for T9, suggesting stronger guest–host interactions between alkanes and the walls of zeolite at the T4 position. This finding suggests that alkanes may prefer to adsorb at the T4 site at low temperatures due to better energy stabilization. On the other hand, at high temperatures, alkanes may prefer to adsorb at the less confined T9 site because of smaller entropy loss for adsorption. However, in practice, the adsorption position is determined not only by temperature but also by the Al distribution, as the distribution of Al in zeolites is often not random and is influenced by the synthesis conditions [48].
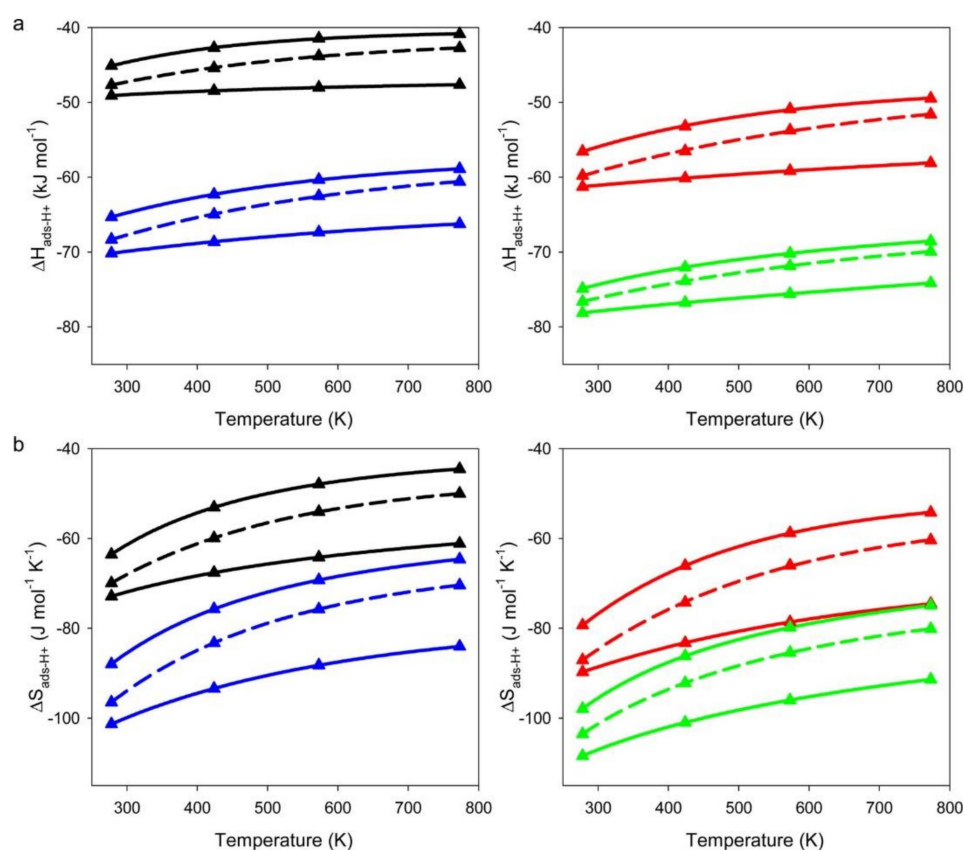


**Figure 1.** CBMC simulations of (**a**) adsorption enthalpies ($\Delta H^{\ddagger}_{ads}$) and (**b**) adsorption entropies ($\Delta S^{\ddagger}_{ads}$) of propane (black triangles), butane (red triangles), pentane (blue triangles), and hexane (green triangles). The upper and lower solid lines represent acid sites located at T9 and T4, respectively. Boltzmann weighted averages of $\Delta H^{\ddagger}_{ads}$ and $\Delta S^{\ddagger}_{ads}$ for Al distributed evenly between T9 and T4 are illustrated as dashed lines. Reprinted with permission from [13]. Copyright 2015, American Chemical Society.

Yang et al. investigated the influence of Al distributions on alkane adsorptions in MFI, TON, FER, MWW, MOR, KFI, and FAU with various Si/Al ratios [14]. They studied the central-to-terminal bond adsorption selectivity ratio of C4-C6 alkanes and found that the influence of Si/Al ratios on the selectivity is negligible. However, their results suggested that the adsorption selectivity ratio is sensitive to Al distributions, because a high selectivity to central bond adsorption was obtained at the T-sites located in a more confined space. In addition, the close spatial proximity of individual Al atoms was also found to enhance the adsorption of central C–C bonds, which indicates that the adsorption selectivity can be tuned by varying the spatial proximity of Al.

Many studies have suggested that the intrinsic activation energy of alkane cracking is not sensitive to zeolite structures [6,7,15–18]. For instance, Van Bokhoven and Xu investigated the rate of monomolecular cracking in MFI, MOR, FAU, and BEA [15], and reported that cracking rates increase with decreasing pore size, but intrinsic activation energies are independent of zeolite structures. Gounder and Iglesia observed similar results when they investigated the intrinsic rate parameters of monomolecular cracking and dehydrogenation of propane in H-MFI, H-FER and H-MOR [16]. They found that the intrinsic activation barriers were similar for these zeolites, in agreement with the study of propane cracking in H-MFI, H-MOR, H-BEA, and H-FAU by Xu et al. [6]. This conclusion is also consistent with the calculations of intrinsic activation barriers for monomolecular propane cracking in zeolites with different topologies (FAU, BEA, MOR, MFI, MWW, and FER) [7]. A similar conclusion was drawn by Kadam et al. when they investigated monomolecular cracking of propane and butane in FER, TON, MFI, and CHA at various temperatures (580–710 K) [17]. These authors found that the activation energies are insensitive to zeolite structures, though the activation entropies increase significantly with the decrease of the zeolite effective radii, suggesting that the confinement affects the entropy of the adsorbed state more significantly than that of the transition state. Recently, Berger et al. employed a hybrid quantum mechanics:quantum mechanics (QM:QM) method, MP2:(PBE + D2) + $\Delta$CCSD(T), in periodic systems to predict the adsorption and activation energies of propane in H-FER, H-MFI, and H-CHA, and concluded that the intrinsic activation enthalpy is insensitive to zeolite structures [18]. To summarize, for the zeolite catalysts discussed above, the intrinsic catalytic activity for cracking is structure-insensitive when considering intrinsic activation energies, and the change of apparent kinetics with different pore sizes and structures can be mainly attributed to the adsorption thermodynamics.

Although the studies discussed above suggested that the intrinsic activation energy for cracking was structure-insensitive, recent investigations indicate that the intrinsic kinetics of cracking may differ between different T-sites for some zeolite systems [8,19], which implies that local porous environments can influence not only the thermodynamics of adsorption but also the intrinsic catalytic activity for cracking. To mitigate this gap between different observations, Bell and co-workers investigated the influence of zeolite structures on monomolecular cracking and dehydrogenation kinetics of butane on various zeolites, including TON, FER, SVR, MFI, MEL, STF, and MWW (Figure 2) [9]. Using the calculated $\Delta S_{ads}^{\ddagger}$ as a descriptor of the degree of confinement in zeolites, they showed that $\Delta H_{int}^{\ddagger}$ and $\Delta S_{int}^{\ddagger}$ for terminal cracking and dehydrogenation decrease with increasing confinements of acid sites, while $\Delta S_{int}^{\ddagger}$ increases and $\Delta H_{int}^{\ddagger}$ remains nearly constant for central cracking. The variations in the intrinsic activation parameters of different reaction pathways suggest that it is possible to achieve high selectivity for the desired product by carefully choosing a zeolite with proper pore sizes. Recently, the same group used a QM/MM approach to calculate intrinsic and apparent activation parameters, and applied thermal adjustments to the apparent barriers derived from CBMC simulations to account for the changes in activation parameters shown in the experiment [10]. They investigated butane cracking in three groups of zeolites that feature different cage sizes or channel patterns. Similar to their previous works, they observed that the variations in reaction paths result in different trends of activation parameters with zeolite topologies. This finding does not support the conclusion drawn by previous studies that intrinsic activation parameters are structure-insensitive and pore topologies only affect adsorption thermodynamics [6,7,15–18]. The discrepancy of the conclusions drawn by different works leaves the effect of local porous environments for intrinsic cracking activity an open question requiring further investigation.
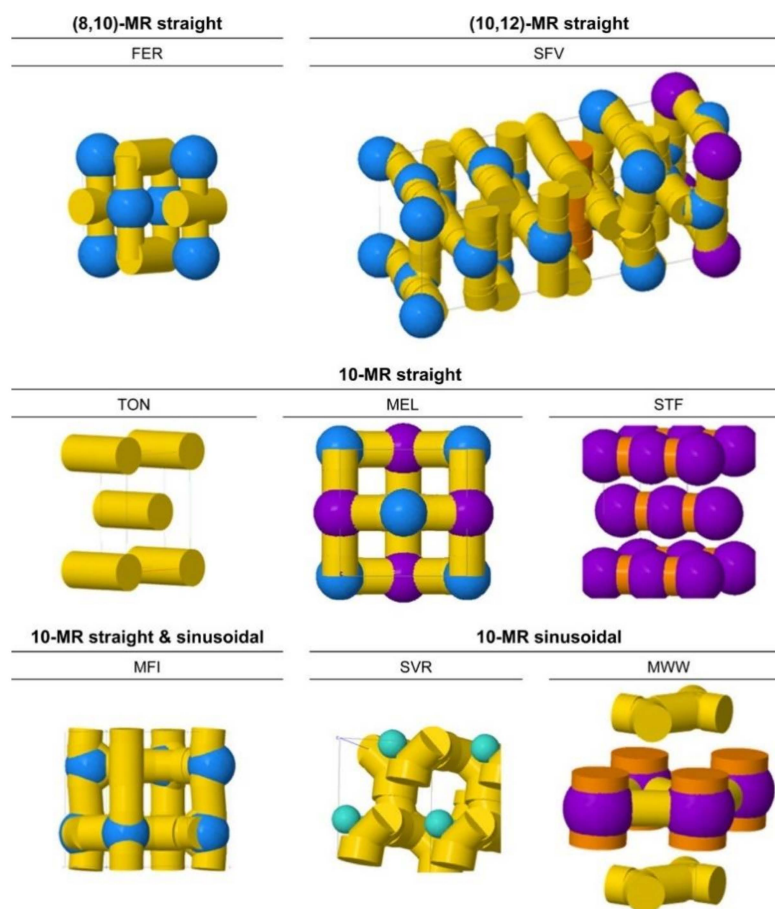
**Figure 2.** Characterizations of 10-membered ring (MR) zeolites with different channel and cavity topologies (generated with the ZEOMICS web tool [49]). Channels are represented in yellow (<6 Å diameter) and orange (>6 Å diameter), while cages are illustrated as green (<6 Å diameter), blue (6–8 Å diameter), and purple (>8 Å diameter) spheres. Reprinted with permission from [9]. Copyright 2016, American Chemical Society.

## 3. The Effects of Mesoporosity on Alkane Cracking

Zeolites have been widely used in the petrochemical industry due to the advantage of excellent hydrothermal stability, strong Brønsted acidity, and shape selectivity. However, microporous zeolites with long diffusion paths experience strong diffusion limitation. This problem manifests itself in two scenarios. The first is that large molecules may not be able to diffuse through the channels to react with an active site. The second is that the cracking products would be stuck in the micropores due to diffuse limitation, and further be over-cracked into undesired byproducts, which could lead to coke formation and the subsequent deactivation of the catalyst.

One way to address this problem is to implement larger pores in zeolites [24–28]. Previous works have successfully fabricated hierarchical zeolites with mesopores of 2–50 nm in diameter with high hydrothermal stability, strong acidity, and low diffusion limitation [26]. In general, mesoporosity can be created using either the top-down or bottom-up methods. The top-down approach is to remove silica or aluminum from the zeolite framework via dealumination or desilication. The drawback of this approach is that it may suffer material loss and it is difficult to control mesoporosity using the top-down approach [26]. These issues can be avoided by using bottom-up methods, which use templates to generate ordered mesoporous structures in the synthesis process. However, the bottom-up method is often more costly than the top-down dealumination/desilication method, and therefore may not be economically feasible for large-scale production [26]. Noteworthy is that the surfactant-templated top-down method can introduce uniformly

distributed mesopores into zeolites, while maintaining the high hydrothermal stability and strong Brønsted acidity, and does not suffer from the drawbacks of material loss and damage of catalyst [24]. In comparison to conventional zeolites, zeolites with secondary porosity display better catalytic performance and longer catalyst lifetime. For instance, mesoporous zeolite Y has been tested in the cracking of vacuum gas oil (VGO). The result showed mesoporous Y produced less coke and more gasoline and light cycle oil (LCO) compared to conventional Y zeolite.

Molecule dynamics (MD) simulations have been applied to study the diffusion of molecules in zeolites at different operation conditions. For instance, Bail et al. investigated the diffusion of hexane in hierarchical mesoporous H-ZSM-5 from 363 K to 543 K using MD simulation and their results indicated that the diffusivity of hexane in a mesostructured zeolite can be higher than in a conventional zeolite at high loading or elevated temperatures [50]. However, diffusing along the mesopore surface at low loading leads to more tortuous diffusion paths, which may cause a reduction in diffusivity. Bu et al. [51] when they investigated the diffusivities of coke precursors such as benzene, naphthalene, and anthracene in mesoporous H-ZSM-5 using MD simulations [47]. They found that these molecules mainly diffuse through micropores or along the external surface of mesoporous zeolites at low temperature, while diffusing along mesopores at pyrolysis temperatures. Recently, Josephson et al. used Monte Carlo simulations to investigate the adsorptions of furan, hexanoic acid, hexane, decane, tetradecane, and 3,6-diethyloctane in hierarchical mesoporous ZSM-5 [52]. Their simulations demonstrated that as pressure increases, alkanes first fill the micropores, then the surface of mesopores and finally the interior of mesopores. In contrast, furan and hexanoic acid predominately adsorb on the surface of mesopores because of hydrogen bonding interactions between adsorbates and silanol groups. These works demonstrated that various guest–host interactions can affect adsorption sites and diffusion paths in zeolite pores, and hence could potentially influence the overall performance of a zeolite catalyst.

As discussed above, DFT studies have provided valuable insights to zeolite catalysis. However, applying DFT calculations to investigate reactions in mesoporous zeolites is very challenging due to the increased structural complexity. With the presence of both microporous and mesoporous channels, the local environment of active sites can vary dramatically from one position to another, so the number of model systems and reaction pathways that need to be considered for a hierarchical zeolite is often higher than that for a conventional zeolite. For example, to study the effect of hierarchical surfaces on ethanol dehydration, Shetsiri et al. built two different cluster models to represent hierarchical and conventional H-ZSM-5 (shown in Figure 3), and found that the preferred dehydration mechanism is dependent on the model system used [53]. Based on both experiments and DFT calculations, these authors demonstrated that direct dehydration of ethanol to form ethylene possibly occurs over the active site at the external surface of hierarchical H-MFI (Figure 3a), while the dehydration of two ethanol molecules to form diethyl ether is preferred for the internal acid site of H-MFI (Figure 3b). This finding highlights the importance of incorporating a significant part of the zeolite structure into the model. Although the use of a simplified model can reduce computational costs, a small or medium model cannot fully describe the effects of confinement and dispersion effects in porous structures [43], which can significantly influence reaction kinetics in zeolites. Recent developments in quantum mechanics/molecular mechanics simulations offer an efficient way to solve this problem [44]. In the QM/MM hybrid scheme, only a small cluster encompassing the active center is described by quantum mechanics, while the rest of the zeolite is described by a classical force field. The QM/MM scheme allows the simulation of reactions in porous environments without significantly increasing computational costs [54–56], and hence may be used increasingly to model complex mesoporous zeolites in the future.
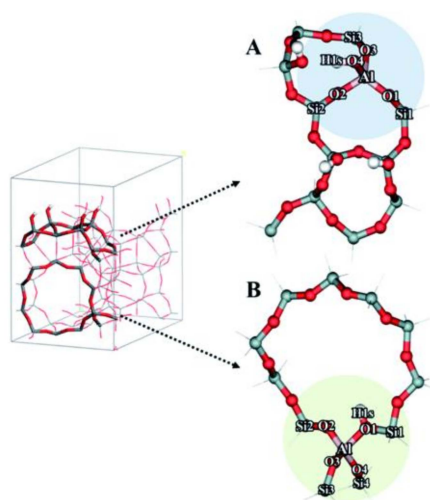
**Figure 3.** The optimized cluster models of (**A**) hierarchical H-ZSM-5 and (**B**) conventional H-ZSM-5. Reproduced from Ref. [53] with permission from the Royal Society of Chemistry.

## 4. Different Active Sites in Zeolites

Zeolites containing different heteroatoms exhibit different catalytic activities [57–60]. If trivalent atoms such as Al substitute for Si in a framework and the charge compensation is provided by protons, Brønsted acid sites are generated in the zeolite pores. In principle, the acidities of these sites are determined by the identity and positions of heteroatoms. Recent studies have also shown that the presence of extra-framework species (often generated after postsynthesis hydrothermal treatments) can also influence the activity of nearby Brønsted acid centers, and therefore could affect cracking activity of a zeolite.

In this section, the results of recent experimental and computational studies related to cracking reactions over different active sites in zeolites are reviewed. This survey begins with Brønsted acid sites in conventional zeolites, followed by a discussion of the synergetic effects between extra-framework species and Brønsted acid sites.

### 4.1. Brønsted Acid Sites in Conventional Zeolites

Though it is well known that Brønsted acid zeolites are active for cracking reactions, identifying the positions of acid sites and controlling their distribution in zeolites remain very challenging. Studies have shown that the distribution of Al atoms in a zeolite is affected by both the Si/Al ratio and the synthesis method [16,48], which may lead to different catalytic activities for the same type of zeolite framework. Therefore, comparing the experimental data reported by different groups should be carried out with care if their zeolites were derived from different sources.

The influence of Si/Al ratio on the distribution of framework Al and its effect on butane cracking and dehydrogenation in H-MFI have been investigated by Janda and Bell [8]. They found that the Brønsted protons are preferably located at channel intersections as the Al content increases. Since the transition state geometry for dehydrogenation is bulky and requires more space than that for cracking reactions, the preference for dehydrogenation to occur at channel interactions is higher than that of cracking to occur. Therefore, the product selectivity of alkane cracking and dehydration could be modified by changing the Si/Al ratio of the zeolite. In addition to the confinement effects, the locations of the protons can also affect the acid properties. Jones et al. performed theoretical simulations to calculate deprotonation energies (DPE) at different T-sites located in various zeolites (MFI, BEA, MOR, FER, FAU, and CHA) [61]. DPE is the energy required to remove a proton from a Brønsted acid site so it can be used to characterize the intrinsic acid strength. Based on the results of Jones et al., DPE values can differ by up to 77 kJ/mol among different T-sites for the zeolites they considered. Since there is a linear relationship

between alkane cracking activity and Brønsted acidity [20–22], the selectivity to cracking products can be turned by acid strength distribution [23].

The Brønsted acidity of zeolites can be modified by the incorporation of various heteroatoms. Among the zeolites substituted with trivalent elements, the strength of Brønsted acid is in the decreasing order of Al-ZSM-5 > Ga-ZSM-5 > B-ZSM-5 [62]. Moreover, the incorporation of alkali, alkaline earth (Na, Mg, K, and Ca), rare earth (La, and Ce), transition metals (Zn, Co, Cu, and Ni), phosphorus and so forth can also influence acid properties [11]. Rahimi et al. have investigated the effect of different promoters on the chemical properties of zeolites and on the catalytic activity and selectivity to light olefins [11]. The incorporation of alkaline and rare earth elements in zeolite can reduce the readsorption of cracking products and promote dehydrogenation, which can improve the yields of light olefins [63–65]. On the other hand, the addition of transition metals can improve dehydrogenative cracking thus improve the yields of light olefins [66]. Besides, the phosphorus-modified ZSM-5 can change the number of acid sites, and Lewis/Brønsted sites ratio, leading to the higher yield of light olefin [67]. Recently, gold catalysts have drawn more attention because of their high catalytic activity at low temperature and high selectivity toward desired products. The cracking of octane and light diesel oil over modified ZSM-5 with gold and lanthanum at 460 °C has been investigated by Liu et al. [68]. Their work found that the incorporation of rare earth $La_2O_3$ into the Au/ZSM-5 catalyst can stabilize Au nanoparticles and meanwhile significantly increase both the selectivity of propylene and the reactive activity. In addition, it was reported that a smaller size of Au particles can provide a better catalytic activity for cracking reactions [69].

*4.2. Extra-Framework Species*

Extra-framework species act as Lewis sites and have synergy with neighboring Brønsted sites [38]. Different metal substituted zeolites have different stability, hence they have different degrees of potential to cause migration of framework metals to extra-framework positions. Since the Ga- or Fe-substituted zeolites are less stable than Al-substituted zeolites, framework Ga and Fe can migrate to extra-framework locations more easily under hydrothermal treatments. Periodic DFT calculations show that the mononuclear oxygenated extra-framework cations are less stable than bi- or multinuclear cationic complexes in Ga-, Zn-, Al-, Cu-, and Fe-modified MOR and ZSM-5 zeolites [70]. Among different extra-framework species, the extra-framework aluminum species are the most studied ones.

It was proposed that the enhanced catalytic performance with the presence of extra-framework species is related to the synergistic effect between EFAL species and vicinal Brønsted acid sites [38]. The Brønsted/Lewis synergy in dealuminated HY zeolites was investigated using solid-state NMR and DFT calculations, and the results from 2-$^{13}$C-acetone NMR and theoretical simulations revealed that the EFAL species can enhance the acid strength of Brønsted acid sites in close proximity to the EFAL species [38]. Alternatively, Gounder et al. proposed that the presence of bulker EFAL species may decrease the effective supercage void sizes, resulting in better stabilization of the transition states [40].

Although it is difficult to identify the structures of EFAL species in zeolites, various mononuclear EFAL species such as $Al^{3+}$, $AlO^+$, $Al(OH)_2^+$, $AlOH^{2+}$, AlOOH, and $Al(OH)_3$ have been proposed. The EFAL species of $Al(OH)_3$ and $Al(OH)_2^+$ have been recognized in dealuminated HY zeolites using $^1$H double quantum magic-angle spinning (DQ-MAS) NMR and DFT calculations [38]. Furthermore, the process of dealumination of HY zeolites was investigated using $^{27}$Al DQ-MAS NMR and DFT calculations, which revealed that the EFAL species of $Al(OH)_3$, $Al(OH)_2^+$, and $AlOH^{2+}$ (in the form of six, five, and four coordination) were the preferred extra-framework species in dealuminated HY zeolites [71]. Similarly, the six-coordinated $Al(OH)_3$ and five-coordinated $AlOH^{2+}$ were identified as the preferred EFAL species in dealuminated H-ZSM-5 and H-MOR zeolites [72]. In combination with DFT calculations and $^{31}$P solid-state NMR using trimethylphosphine as a probe molecule, the origin, structure, and the possible locations of tri-coordinated EFAL-$Al^{3+}$ moieties in dealuminated HY zeolites were investigated [39,73]. Apart from mononuclear

EFAL species, multinuclear counterparts could also form in zeolites. For instance, the presence of tri- and tetranuclear EFAL species inside the sodalite cage of faujasite zeolite was reported by Liu et al. by using periodic DFT calculations [37]. Their ab initio thermodynamic analysis suggested that the multinuclear cationic complexes were the dominant EFAL complexes under realistic conditions. Such self-aggregation was also found in La-FAU [74]. Recently, the presence of multinuclear EFAL species in dealuminated zeolites was measured for the first time in experiments using the combined $^{31}$P solid-state NMR and 1,2-bis(dimethylphosphine) ethane probe molecule method [75].

The beneficial effect of extra-framework species is well known for the enhancement of acidity, which improves catalytic performance of cracking reactions [5,29,34–42]. For example, the enhanced cracking activity of propane in zeolites Y with more Brønsted acid sites perturbed by EFAL species was investigated by the experiments [5]. This beneficial effect has also been found for cracking reactions in mesoporous zeolites Y [29]. To gain more insight into the effect of EFAL species on cracking reactions, Liu et al. performed periodic DFT calculations of propane cracking over EFAL-free (H-FAU) and EFAL-containing (EFAL/H-FAU) zeolites [37]. Figure 4a shows the models of H-FAU and EFAL/H-FAU, where trinuclear $[Al_3O_4H_3]^{4+}$ was chosen as the EFAL species located inside the sodalite cage. The reaction mechanism of monomolecular propane cracking and the corresponding structures of the reactants, transition states, and intermediates are presented in Figure 4b,c, respectively. As shown in Figure 4d, the presence of EFAL in zeolite can significantly reduce the reaction barrier for propane cracking from 200 to 149 kJ/mol. Furthermore, the stronger stabilization of the transition state and intermediate in EFAL/H-FAU was found due to the charge compensation of the deprotonated oxygen by cationic EFAL. In addition to extra-framework aluminum species, the extra-framework Ga species have been studied recently both experimentally and theoretically for dehydrogenation and cracking reactions in Ga/H-MFI [41,42]. Under the same reaction conditions, the reaction rates for propane dehydrogenation and cracking over Ga/H-MFI are ~500 and ~20 times higher than the corresponding rates over conventional H-MFI.
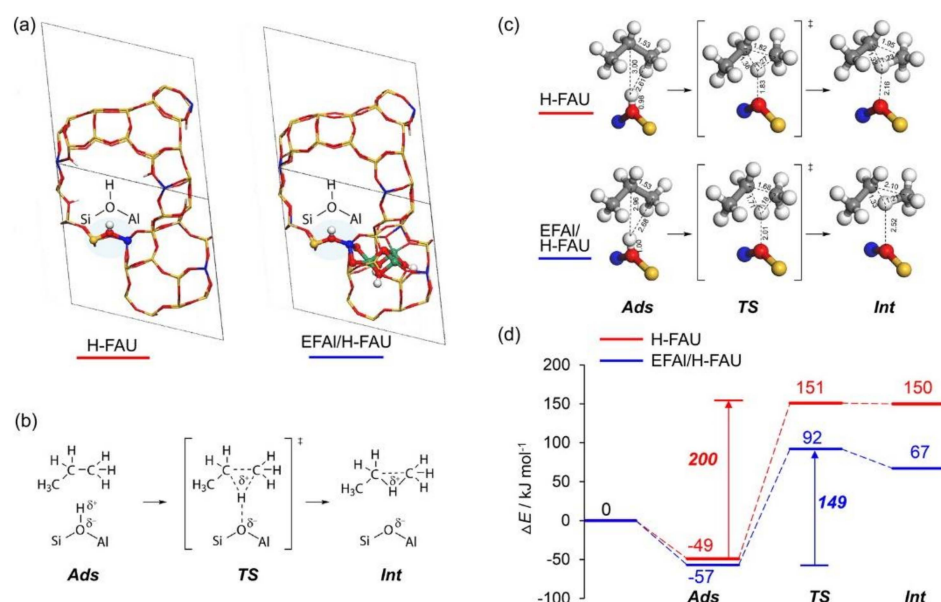


**Figure 4.** (**a**) The models of H-FAU (left) and EFAL/H-FAU (right). (**b**) The reaction mechanism of monomolecular propane cracking to form a carbonium ion intermediate via protonation of C–C bond. (**c**) The structures of reactants, transition states, and intermediates for propane cracking over H-FAU and EFAL/H-FAU. (**d**) The energy diagrams of propane cracking reactions over H-FAU and EFAL/H-FAU. Reprinted with permission from [37]. Copyright 2015, American Chemical Society.

## 5. Conclusions

This review shows the overview of recent theoretical and experimental studies of cracking reactions in mesoporous and microporous zeolites. The adsorption parameters of alkanes in zeolites are structure-sensitive, and the adsorption occurs mainly on less confined acid sites. By contrast, many authors suggested that the intrinsic kinetic parameters are insensitive to zeolite structures, while different results were obtained by using Monte Carlo simulations.

Although conventional zeolites have the advantages of higher surface area, better hydrothermal stability, and superior shape selectivity, they still have a major drawback of diffusion limitation, which can be mitigated by introducing mesopores in zeolites. Experiments have shown that the presence of mesopores can enhance the selectivity to desired products and reduce coke formation. However, systematic theoretical investigations of the influence of mesoporosity on cracking reactions are still lacking, because of the structural complexity of mesoporous catalysts and the high computational cost for modeling such complex systems. Although some works have employed small or medium-sized cluster models to perform mechanistic studies for reactions in hierarchical zeolites, these models cannot fully describe the confinement and dispersion effects in porous structures. One strategy to balance accuracy and computational cost is to use the combined quantum mechanics/molecular mechanics (QM/MM) approach, which allows one to include a significant part of a porous catalyst into the model without greatly increasing the computational costs, and thus is an appealing method for modeling mesoporous zeolites in the future.

In addition to the confinement effect in zeolite pores, studies have shown that the Si/Al ratio, the distribution of Al, and Brønsted acidity also influence alkane cracking in zeolites. However, identifying and controlling the positions of aluminum atoms in zeolites still remain challenging. In addition, extra-framework species generated after postsynthesis hydrothermal treatment have also been shown to enhance the acidity of nearby Brønsted acid sites. Recent studies have proposed many different structures for the extra-framework species in zeolite systems. However, how to engineer these extra-framework species to optimize zeolite activity for cracking is still challenging and requires further investigation.

**Author Contributions:** Conceptualization, S.-C.L.; writing—original draft preparation, S.-C.L., Y.-C.L.; writing—review and editing, Y.-P.L.; supervision, Y.-P.L.; project administration, Y.-P.L. All authors have read and agreed to the published version of the manuscript.

## Abbreviations

| | |
|---|---|
| CBMC | configurational-bias Monte Carlo |
| DFT | density functional theory |
| DPE | deprotonation energy |
| DQ-MAS | double quantum magic-angle spinning |
| EFAL | extra-framework aluminum |
| FCC | fluidized catalytic cracking |
| LCO | light cycle oil |
| MBH | mobile block Hessian |
| MD | molecule dynamics |
| QM/MM | quantum mechanics/molecular mechanics |
| QM:QM | quantum mechanics:quantum mechanics |
| quasi-RRHO | quasi-rigid rotor harmonic oscillator |
| VGO | vacuum gas oil |

# References

1.  Komvokis, V.; Tan, L.X.L.; Clough, M.; Pan, S.S.; Yilmaz, B. Zeolites in fluid catalytic cracking (FCC). In *Zeolites in Sustainable Chemistry*; Springer: Berlin/Heidelberg, Germany, 2016; pp. 271–297.
2.  Bender, M. An overview of industrial processes for the production of olefins—C4Hydrocarbons. *ChemBioEng Rev.* **2014**, *1*, 136–147. [CrossRef]
3.  Gholami, Z.; Gholami, F.; Tišler, Z.; Tomas, M.; Vakili, M. A review on production of light olefins via fluid catalytic cracking. *Energies* **2021**, *14*, 1089. [CrossRef]
4.  Zacharopoulou, V.; Lemonidou, A.A. Olefins from biomass intermediates: A review. *Catalysts* **2017**, *8*, 2. [CrossRef]
5.  Almutairi, S.M.; Mezari, B.; Filonenko, G.A.; Magusin, P.C.; Rigutto, M.S.; Pidko, E.A.; Hensen, E.J. Influence of extraframe-work aluminum on the Brønsted acidity and catalytic reactivity of faujasite zeolite. *ChemCatChem* **2013**, *5*, 452–466. [CrossRef]
6.  Xu, B.; Sievers, C.; Hong, S.B.; Prins, R.; van Bokhoven, J.A. Catalytic activity of Brønsted acid sites in zeolites: Intrinsic activity, rate-limiting step, and influence of the local structure of the acid sites. *J. Catal.* **2006**, *244*, 163–168. [CrossRef]
7.  Jones, A.J.; Zones, S.I.; Iglesia, E. Implications of transition state confinement within small voids for acid catalysis. *J. Phys. Chem. C* **2014**, *118*, 17787–17800. [CrossRef]
8.  Janda, A.; Bell, A. Effects of Si/Al ratio on the distribution of framework Al and on the rates of alkane monomolecular cracking and dehydrogenation in H-MFI. *J. Am. Chem. Soc.* **2013**, *135*, 19193–19207. [CrossRef]
9.  Janda, A.; Vlaisavljevich, B.; Lin, L.-C.; Smit, B.; Bell, A.T. Effects of zeolite structural confinement on adsorption thermodynamics and reaction kinetics for monomolecular cracking and dehydrogenation of n-butane. *J. Am. Chem. Soc.* **2016**, *138*, 4739–4756. [CrossRef]
10. Van der Mynsbrugge, J.; Janda, A.; Sharada, S.M.; Lin, L.-C.; Van Speybroeck, V.; Head-Gordon, M.; Bell, A.T. Theoretical analysis of the influence of pore geometry on monomolecular cracking and dehydrogenation of n-butane in Brønsted acidic zeolites. *ACS Catal.* **2017**, *7*, 2685–2697. [CrossRef]
11. Rahimi, N.; Karimzadeh, R. Catalytic cracking of hydrocarbons over modified ZSM-5 zeolites to produce light olefins: A review. *Appl. Catal. A Gen.* **2011**, *398*, 1–17. [CrossRef]
12. Blay, V.; Louis, B.; Miravalles, R.; Yokoi, T.; Peccatiello, K.A.; Clough, M.; Yilmaz, B. Engineering zeolites for catalytic cracking to light olefins. *ACS Catal.* **2017**, *7*, 6542–6566. [CrossRef]
13. Janda, A.; Vlaisavljevich, B.; Lin, L.-C.; Mallikarjun Sharada, S.; Smit, B.; Head-Gordon, M.; Bell, A.T. Adsorption thermo-dynamics and intrinsic activation parameters for monomolecular cracking of n-alkanes on Brønsted acid sites in zeolites. *J. Phys. Chem. C* **2015**, *119*, 10427–10438. [CrossRef]
14. Yang, C.-T.; Janda, A.; Bell, A.T.; Lin, L.-C. Atomistic investigations of the effects of Si/Al ratio and Al distribution on the adsorption selectivity of n-alkanes in Brønsted-acid zeolites. *J. Phys. Chem. C* **2018**, *122*, 9397–9410. [CrossRef]
15. Van Bokhoven, J.A.; Xu, B. Towards predicting catalytic performances of zeolites. In *Studies in Surface Science and Catalysis*; Elsevier: Amsterdam, The Netherlands, 2007; Volume 170, pp. 1167–1173.
16. Gounder, R.; Iglesia, E. Catalytic consequences of spatial constraints and acid site location for monomolecular alkane activation on zeolites. *J. Am. Chem. Soc.* **2009**, *131*, 1958–1971. [CrossRef]
17. Kadam, S.A.; Li, H.; Wormsbecher, R.F.; Travert, A. Impact of zeolite structure on entropic-enthalpic contributions to alkane monomolecular cracking: An IR operando study. *Chem. Eur. J.* **2018**, *24*, 5489–5492. [CrossRef]
18. Berger, F.; Rybicki, M.; Sauer, J. Adsorption and cracking of propane by zeolites of different pore size. *J. Catal.* **2021**, *395*, 117–128. [CrossRef]
19. Mallikarjun Sharada, S.; Zimmerman, P.M.; Bell, A.T.; Head-Gordon, M. Insights into the kinetics of cracking and dehydro-genation reactions of light alkanes in H-MFI. *J. Phys. Chem. C* **2013**, *117*, 12600–12611. [CrossRef]
20. Niwa, M.; Suzuki, K.; Morishita, N.; Sastre, G.; Okumura, K.; Katada, N. Dependence of cracking activity on the Brønsted acidity of Y zeolite: DFT study and experimental confirmation. *Catal. Sci. Technol.* **2013**, *3*, 1919–1927. [CrossRef]
21. Borges, P.; Pinto, R.R.; Lemos, M.A.; Lemos, F.; Védrine, J.; Derouane, E.; Ribeiro, F.R. Activity–acidity relationship for alkane cracking over zeolites: N-hexane cracking over HZSM-5. *J. Mol. Catal. A Chem.* **2005**, *229*, 127–135. [CrossRef]
22. Katada, N.; Sota, S.; Morishita, N.; Okumura, K.; Niwa, M. Relationship between activation energy and pre-exponential factor normalized by the number of Brønsted acid sites in cracking of short chain alkanes on zeolites. *Catal. Sci. Technol.* **2014**, *5*, 1864–1869. [CrossRef]
23. Lin, L.; Qiu, C.; Zhuo, Z.; Zhang, D.; Zhao, S.; Wu, H.; Liu, Y.; He, M. Acid strength controlled reaction pathways for the catalytic cracking of 1-butene to propene over ZSM-5. *J. Catal.* **2013**, *309*, 136–145. [CrossRef]
24. Garcia-Martinez, J.; Johnson, M.M.; Valla, J.; Li, K.; Ying, J. Mesostructured zeolite Y—High hydrothermal stability and superior FCC catalytic performance. *Catal. Sci. Technol.* **2012**, *2*, 987–994. [CrossRef]
25. Choi, M.; Na, K.; Kim, J.; Sakamoto, Y.; Terasaki, O.; Ryoo, R. Stable single-unit-cell nanosheets of zeolite MFI as active and long-lived catalysts. *Nature* **2009**, *461*, 246–249. [CrossRef]
26. Li, K.; Valla, J.; Garcia-Martinez, J. Realizing the commercial potential of hierarchical zeolites: New opportunities in catalytic cracking. *ChemCatChem* **2013**, *6*, 46–66. [CrossRef]
27. Srivastava, R. Synthesis and applications of ordered and disordered mesoporous zeolites: Present and future prospective. *Catal. Today* **2018**, *309*, 172–188. [CrossRef]

28. Peng, P.; Gao, X.-H.; Yan, Z.-F.; Mintova, S. Diffusion and catalyst efficiency in hierarchical zeolite catalysts. *Natl. Sci. Rev.* **2020**, *7*, 1726–1742. [CrossRef]

29. Chapellière, Y.; Daniel, C.; Tuel, A.; Farrusseng, D.; Schuurman, Y. Kinetics of n-hexane cracking over mesoporous HY zeolites based on catalyst descriptors. *Catalysts* **2021**, *11*, 652. [CrossRef]

30. Zhou, F.; Gao, Y.; Wu, G.; Ma, F.; Liu, C. Improved catalytic performance and decreased coke formation in post-treated ZSM-5 zeolites for methanol aromatization. *Microporous Mesoporous Mater.* **2017**, *240*, 96–107. [CrossRef]

31. Zhao, T.; Li, F.; Yu, H.; Ding, S.; Li, Z.; Huang, X.; Li, X.; Wei, X.; Wang, Z.; Lin, H. Synthesis of mesoporous ZSM-5 zeolites and catalytic cracking of ethanol and oleic acid into light olefins. *Appl. Catal. A Gen.* **2019**, *575*, 101–110. [CrossRef]

32. Khalil, U.; Liu, Z.; Peng, C.; Hikichi, N.; Wakihara, T.; García-Martínez, J.; Okubo, T.; Bhattacharya, S. Ultrafast surfactant-templating of BEA zeolite: An efficient catalyst for the cracking of polyethylene pyrolysis vapours. *Chem. Eng. J.* **2021**, *412*, 128566. [CrossRef]

33. Pala-Rosas, I.; Contreras, J.; Salmones, J.; Zeifert, B.; López-Medina, R.; Navarrete-Bolaños, J.; Hernández-Ramírez, S.; Pérez-Cabrera, J.; de Oca, A.F.-M. Catalytic deactivation of HY zeolites in the dehydration of glycerol to acrolein. *Catalysts* **2021**, *11*, 360. [CrossRef]

34. Zhang, Y.; Zhao, R.; Sanchez, M.; Haller, G.L.; Hu, J.; Bermejo-Deval, R.; Liu, Y.; Lercher, J.A. Promotion of protolytic pentane conversion on H-MFI zeolite by proximity of extra-framework aluminum oxide and Brønsted acid sites. *J. Catal.* **2019**, *370*, 424–433. [CrossRef]

35. Mezari, B.; Magusin, P.C.; Almutairi, S.M.; Pidko, E.A.; Hensen, E.J. Nature of enhanced Brønsted acidity induced by extraframework aluminum in an ultrastabilized faujasite zeolite: An in situ NMR study. *J. Phys. Chem. C* **2021**, *125*, 9050–9059. [CrossRef]

36. Li, G.; Pidko, E.A. The nature and catalytic function of cation sites in zeolites: A computational perspective. *ChemCatChem* **2018**, *11*, 134–156. [CrossRef]

37. Liu, C.; Li, G.; Hensen, E.J.M.; Pidko, E.A. Nature and catalytic role of extraframework aluminum in faujasite zeolite: A theoretical perspective. *ACS Catal.* **2015**, *5*, 7024–7033. [CrossRef]

38. Li, S.; Zheng, A.; Su, Y.; Zhang, H.; Chen, L.; Yang, J.; Ye, A.C.; Deng, F. Brønsted/Lewis acid synergy in dealuminated HY zeolite: A combined solid-state NMR and theoretical calculation study. *J. Am. Chem. Soc.* **2007**, *129*, 11161–11171. [CrossRef] [PubMed]

39. Liu, C.; Li, G.; Hensen, E.J.; Pidko, E.A. Relationship between acidity and catalytic reactivity of faujasite zeolite: A periodic DFT study. *J. Catal.* **2016**, *344*, 570–577. [CrossRef]

40. Gounder, R.; Jones, A.J.; Carr, R.T.; Iglesia, E. Solvation and acid strength effects on catalysis by faujasite zeolites. *J. Catal.* **2012**, *286*, 214–223. [CrossRef]

41. Phadke, N.M.; Mansoor, E.; Bondil, M.; Head-Gordon, M.; Bell, A.T. Mechanism and kinetics of propane dehydrogenation and cracking over Ga/H-MFI prepared via vapor-phase exchange of H-MFI with GaCl$_3$. *J. Am. Chem. Soc.* **2018**, *141*, 1614–1627. [CrossRef] [PubMed]

42. Phadke, N.M.; Mansoor, E.; Head-Gordon, M.; Bell, A.T. Mechanism and kinetics of light alkane dehydrogenation and cracking over isolated Ga species in Ga/H-MFI. *ACS Catal.* **2021**, *11*, 2062–2075. [CrossRef]

43. Yeh, J.Y.; Li, S.C.; Chen, C.H.; Wu, K.C.W.; Li, Y.P. Quantum mechanical calculations for biomass valorization over Metal-Organic Frameworks (MOFs). *Chem. Asian J.* **2021**, *16*, 1049–1056. [CrossRef]

44. Li, Y.-P.; Gomes, J.; Mallikarjun Sharada, S.; Bell, A.T.; Head-Gordon, M. Improved force-field parameters for QM/MM simulations of the energies of adsorption for molecules in zeolites and a free rotor correction to the rigid rotor harmonic oscillator model for adsorption enthalpies. *J. Phys. Chem. C* **2015**, *119*, 1840–1850. [CrossRef]

45. Li, Y.-P.; Bell, A.T.; Head-Gordon, M. Thermodynamics of anharmonic systems: Uncoupled mode approximations for molecules. *J. Chem. Theory Comput.* **2016**, *12*, 2861–2870. [CrossRef] [PubMed]

46. Ghysels, A.; Van Neck, D.; Van Speybroeck, V.; Verstraelen, T.; Waroquier, M. Vibrational modes in partially optimized molecular systems. *J. Chem. Phys.* **2007**, *126*, 224102. [CrossRef]

47. Grimme, S. Supramolecular binding thermodynamics by dispersion-corrected density functional theory. *Chem. Eur. J.* **2012**, *18*, 9955–9964. [CrossRef] [PubMed]

48. Sklenak, S.; Dedecek, J.; Li, C.; Wichterlova, B.; Gábová, V.; Sierka, M.; Sauer, J. Aluminium siting in the ZSM-5 framework by combination of high resolution 27Al NMR and DFT/MM calculations. *Phys. Chem. Chem. Phys.* **2009**, *11*, 1237–1247. [CrossRef] [PubMed]

49. First, E.L.; Gounaris, C.; Wei, J.; Floudas, C.A. Computational characterization of zeolite porous networks: An automated approach. *Phys. Chem. Chem. Phys.* **2011**, *13*, 17339–17358. [CrossRef]

50. Bai, P.; Haldoupis, E.; Dauenhauer, P.J.; Tsapatsis, M.; Siepmann, J.I. Understanding diffusion in hierarchical zeolites with house-of-cards nanosheets. *ACS Nano* **2016**, *10*, 7612–7618. [CrossRef]

51. Bu, L.; Nimlos, M.R.; Robichaud, D.J.; Kim, S. Diffusion of aromatic hydrocarbons in hierarchical mesoporous H-ZSM-5 zeolite. *Catal. Today* **2018**, *312*, 73–81. [CrossRef]

52. Josephson, T.R.; Dauenhauer, P.J.; Tsapatsis, M.; Siepmann, J.I. Adsorption of furan, hexanoic acid, and alkanes in a hierarchical zeolite at reaction conditions: Insights from molecular simulations. *J. Comput. Sci.* **2021**, *48*, 101267. [CrossRef]

53. Shetsiri, S.; Thivasasith, A.; Saenluang, K.; Wannapakdee, W.; Salakhum, S.; Wetchasat, P.; Nokbin, S.; Limtrakul, J.; Wattanakit, C. Sustainable production of ethylene from bioethanol over hierarchical ZSM-5 nanosheets. *Sustain. Energy Fuels* **2018**, *3*, 115–126. [CrossRef]

54. Li, Y.-P.; Head-Gordon, M.; Bell, A. Analysis of the reaction mechanism and catalytic activity of metal-substituted beta zeolite for the isomerization of glucose to fructose. *ACS Catal.* **2014**, *4*, 1537–1545. [CrossRef]

55. Li, Y.-P.; Head-Gordon, M.; Bell, A.T. Computational study of p-Xylene synthesis from ethylene and 2,5-dimethylfuran catalyzed by H-BEA. *J. Phys. Chem. C* **2014**, *118*, 22090–22095. [CrossRef]

56. Li, Y.-P.; Head-Gordon, M.; Bell, A.T. Theoretical study of 4-(hydroxymethyl) benzoic acid synthesis from ethylene and 5-(hydroxymethyl) furoic acid catalyzed by Sn-BEA. *ACS Catal.* **2016**, *6*, 5052–5061. [CrossRef]

57. Ji, Y.; Shi, B.; Yang, H.; Yan, W. Synthesis of isomorphous MFI nanosheet zeolites for supercritical catalytic cracking of n-dodecane. *Appl. Catal. A Gen.* **2017**, *533*, 90–98. [CrossRef]

58. Qin, F.; Wang, Y.; Lu, Y.; Osuga, R.; Gies, H.; Kondo, J.N.; Yokoi, T. Synthesis of novel aluminoborosilicate isomorphous to zeolite TUN and its acidic and catalytic properties. *Microporous Mesoporous Mater.* **2021**, *323*, 111237. [CrossRef]

59. Yabushita, M.; Osuga, R.; Muramatsu, A. Control of location and distribution of heteroatoms substituted isomorphously in framework of zeolites and zeotype materials. *CrystEngComm* **2021**. [CrossRef]

60. Yabushita, M.; Kobayashi, H.; Neya, A.; Nakaya, M.; Maki, S.; Matsubara, M.; Kanie, K.; Muramatsu, A. Precise control of density and strength of acid sites of MFI-type zeolite nanoparticles via simultaneous isomorphous substitution by Al and Fe. *CrystEngComm* **2020**, *22*, 7556–7564. [CrossRef]

61. Jones, A.J.; Iglesia, E. The strength of Brønsted acid sites in microporous aluminosilicates. *ACS Catal.* **2015**, *5*, 5741–5755. [CrossRef]

62. Jungsuttiwong, S.; Lomratsiri, J.; Limtrakul, J. Characterization of acidity in [B], [Al], and [Ga] isomorphously substituted ZSM-5: Embedded DFT/UFF approach. *Int. J. Quantum Chem.* **2011**, *111*, 2275–2282. [CrossRef]

63. Yoshimura, Y.; Kijima, N.; Hayakawa, T.; Murata, K.; Suzuki, K.; Mizukami, F.; Matano, K.; Konishi, T.; Oikawa, T.; Saito, M.; et al. Catalytic cracking of naphtha to light olefins. *Catal. Surv. Jpn.* **2001**, *4*, 157–167. [CrossRef]

64. Wakui, K.; Satoh, K.; Sawada, G.; Shiozawa, K.; Matano, K.; Suzuki, K.; Hayakawa, T.; Yoshimura, Y.; Murata, K.; Mizukami, F. Dehydrogenative Cracking of n-butane over modified HZSM-5 catalysts. *Catal. Lett.* **2002**, *81*, 83–88. [CrossRef]

65. Xiaoning, W.; Zhen, Z.; Chunming, X.; Aijun, D.; Li, Z.; Guiyuan, J. Effects of light rare earth on acidity and catalytic per-formance of HZSM-5 zeolite for catalytic cracking of butane to light olefins. *J. Rare Earths* **2007**, *25*, 321–328. [CrossRef]

66. Sun, Y.; Brown, T.C. Catalytic cracking, dehydrogenation, and aromatization of isobutane over Ga/HZSM-5 and Zn/HZSM-5 at low pressures. *Int. J. Chem. Kinet.* **2002**, *34*, 467–480. [CrossRef]

67. Xue, N.; Chen, X.; Nie, L.; Guo, X.; Ding, W.; Chen, Y.; Gu, M.; Xie, Z. Understanding the enhancement of catalytic performance for olefin cracking: Hydrothermally stable acids in P/HZSM-5. *J. Catal.* **2007**, *248*, 20–28. [CrossRef]

68. Liu, Q.; Zhang, M.; Sun, L.; Su, H.; Zou, X.; Qi, C. The performance of catalytic conversion of ZSM-5 comodified with gold and lanthanum for increasing propylene production. *Ind. Eng. Chem. Res.* **2019**, *58*, 14695–14704. [CrossRef]

69. Zhang, M.; Liu, Q.; Long, H.; Sun, L.; Murayama, T.; Qi, C. Insights into Au nanoparticle size and chemical state of Au/ZSM-5 catalyst for catalytic cracking of n-octane to increase propylene production. *J. Phys. Chem. C* **2021**, *125*, 29. [CrossRef]

70. Pidko, E.A.; Hensen, E.J.M.; Van Santen, R.A. Self-organization of extraframework cations in zeolites. *Proc. R. Soc. A Math. Phys. Eng. Sci.* **2012**, *468*, 2070–2086. [CrossRef]

71. Yu, Z.; Zheng, A.; Wang, Q.; Chen, L.; Xu, J.; Amoureux, J.-P.; Deng, F. Insights into the dealumination of zeolite HY revealed by sensitivity-enhanced 27Al DQ-MAS NMR spectroscopy at high field. *Angew. Chem. Int. Ed.* **2010**, *122*, 8839–8843. [CrossRef]

72. Yu, Z.; Li, S.; Wang, Q.; Zheng, A.; Jun, X.; Chen, L.; Deng, F. Brønsted/Lewis acid synergy in H–ZSM-5 and H–MOR zeolites studied by 1H and 27Al DQ-MAS solid-state NMR spectroscopy. *J. Phys. Chem. C* **2011**, *115*, 22320–22327. [CrossRef]

73. Yi, X.; Liu, K.; Chen, W.; Li, J.; Xu, S.; Li, C.; Xiao, Y.; Liu, H.; Guo, X.; Liu, S.-B.; et al. Origin and structural characteristics of tri-coordinated extra-framework aluminum species in dealuminated zeolites. *J. Am. Chem. Soc.* **2018**, *140*, 10764–10774. [CrossRef] [PubMed]

74. Schüßler, F.; Pidko, E.A.; Kolvenbach, R.; Sievers, C.; Hensen, E.J.M.; van Santen, R.A.; Lercher, J.A. Nature and location of cationic lanthanum species in high alumina containing faujasite type zeolites. *J. Phys. Chem. C* **2011**, *115*, 21763–21776. [CrossRef]

75. Zheng, A.; Yi, X.; Xiao, Y.; Liu, Z.; Li, G.; Chen, W.; Liu, S. Observation of Multinuclear Extra-Framework Aluminum Species in Dealuminated Zeolite Catalysts. Research Square. Available online: https://assets.researchsquare.com/files/rs-50498/v1/0ef491 98-624e-43a3-a79a-b1d936b0bbca.pdf (accessed on 29 August 2021).